Environment Protection Engineering

Vol. 50 2024 No. 1

DOI: 10.37190/epe240102

SHUQIN ZHANG (ORCID: 0000-0002-1572-308X)[1, 2]
BOYUE YUAN (ORCID: 0000-0002-1038-1471)[1]
YI LIU (ORCID: 0009-0001-5358-3110)[1]
KENING ZHANG (ORCID: 0009-0002-5230-1457)[1]
DAJUN REN (ORCID: 0000-0003-0752-4184)[1, 2]
XIAOQING ZHANG (ORCID: 0000-0002-6456-0600)[1, 2]

COMPARATIVE STUDY ON THE ADSORPTION OF LEAD IONS BY KAOLIN LOADED CHITOSAN BY DIFFERENT MODIFICATION METHODS

The adsorption effect of two modified kaolin-chitosan composites prepared by different modification methods (cross-linking method (GL-CS) and click reaction method (TGL-CS) on lead ion wastewater was studied. The structure of TGL-CS has a denser pore structure than that of GL-CS, and the distribution of adsorption sites is more uniform. At 25 °C, pH 4, the adsorbent dosage of 0.05 g/dm^3, reaction time of 4 h, and initial mass concentration of 150 mg/dm^3, TGL-CS had the best effect on Pb^{2+} wastewater treatment, and the adsorption capacity was 76.159 mg/g. The adsorption studies of kinetic, thermodynamic, and thermodynamic parameters showed that the adsorption on GL-CS and TGL-CS was best described by the Langmuir model. The adsorption mechanism is mainly chemical adsorption. The adsorption process is spontaneous. These results show that the adsorbent prepared by click reaction has obvious advantages, with more adsorption capacity and adsorption sites, faster adsorption rate, and better application potential.

1. INTRODUCTION

With the development of industry, heavy metal pollution has become a serious environmental problem worldwide. Lead is one of the most abundant heavy metals found in the earth's crust. Pb and its compounds are important industrial raw materials in modern society and are widely used in various industries such as electroplating, metallurgy,

[1]College of Resources and Environmental Engineering, Wuhan University of Science and Technology, Hubei, China, corresponding author S. Zhang, email address: zhangshuqin@wust.edu.cn

[2]Hubei Key Laboratory for Efficient Utilization and Agglomeration of Metallurgic Mineral Resources, Wuhan University of Science and Technology, Wuhan, China.

and coal combustion. In the industrial process, the waste liquid and waste residue produced contain a large amount of residual Pb [1–3]. As a highly toxic heavy metal, Pb is characterized by easy accumulation, enrichment, long-term, and concealment [4]. Therefore, lead easily enters the human body through agricultural products and other ways of endangering human health and cannot be degraded by microorganisms, and the biological half-life is very long [5]. Thus, the treatment of wastewater containing Pb has attracted extensive attention from researchers.

Heavy metal wastewater treatment methods include chemical precipitation, metal reduction, adsorption, ion exchange, electrolysis, and microbial methods [6]. The adsorption method is widely used because of its high treatment efficiency and simple process, which is one of the main technologies for the treatment of lead-containing wastewater [6–8]. It is a treatment method that uses a large specific surface area and rich pore structure of the adsorbent, as well as chemical functional groups with special functions, such as electrostatic attraction and chemical action to migrate lead ions to the chelating site of the adsorbed substance. These include chemical adsorption, physical adsorption, and biological adsorption. The adsorbent is a key factor in determining whether the technology can be used efficiently, so the research on the adsorbent with efficient utilization has become a research hot topic.

Chitosan, also known as deacetylated chitin, is a rich and common organic compound in nature. Chitosan is easy to obtain and can be completely biodegradable. The molecular structure of chitosan is composed of a large number of active groups, including amino and hydroxyl functional groups, which can effectively chelate with heavy metal ions. The physical properties, hydrophilicity, and high reactivity of chitosan determine its high adsorption capacity for heavy metal ions [9–11]. Therefore, chitosan has been widely used to remove heavy metal ions in wastewater. Kaolin is a rich clay mineral, which is a kind of hexagonal scale crystal. The interlayers of kaolin are closely connected by hydrogen bonding and its molecular structure is relatively stable. It has a large surface area, easy dispersion in water, high adhesion, and high stability [12]. The surface of kaolin is rich in hydroxyl groups, which makes it easy to react with metal cations. The above characteristics make kaolin have strong adsorption potential [13]. Therefore, kaolin is widely used in the field of heavy metal adsorption.

Many studies have focused on the use of different methods to combine chitosan and kaolin to prepare composite materials with high adsorption and large capacity. He et al. [14] synthesized chitosan-kaolin composite hydrogel by cross-linking reaction, and the adsorption capacity was significantly improved. Vedula et al. [15] synthesized a biological composite membrane with chitosan and kaolin and its adsorption removal rate of copper ions reached 86%. As reported by Liu et al. [16], magnetic kaolin-coated chitosan particles were used to prepare composite materials to adsorb Cr(VI) ions. Their adsorption rate was greatly improved. Zhou et al. [17] successfully prepared chitosan-kaolin com-

posite adsorption particles by introducing amino groups in chitosan into the kaolin interlayer, which effectively improved the adsorption of phosphate. These experiments prove that the composite material has superior performance compared to a single material.

In this study, kaolin was loaded on chitosan by two modification methods (cross-linking reaction and click reaction) to prepare a new adsorbent. The adsorption mechanism was determined by comparing the adsorption effects of the adsorbents prepared by the two methods and analyzing the kinetics model, adsorption isotherms, and adsorption thermodynamics.

2. MATERIALS AND METHODS

Materials. Lead(II) nitrate, chitosan, kaolin, glutaraldehyde, anhydrousethanol, 3-mercaptopropyltriethoxysilane, 2-ethylacrolein, dimethylolpropionic acid, tetrahydrofurane, ice acetic acid, sodium hydroxide were all purchased from the Sinopharm Group Chemical Reagents Co., Ltd.

Chitosan/kaolin composite adsorbent (GL-CS) by the crosslinking method. Chitosan-kaolin composite (GL-CS) was prepared by the Schiff base reaction [14]. 0.9 g of chitosan (CS) was dissolved in a certain amount of pure water at 25 °C, so that the content of chitosan was 1 wt.%. Then kaolin (GL) was added to the chitosan solution at a weight ratio of 9:1 and mixed in an ice water bath. 10 cm^3 of 25% glutaraldehyde (GA) was added to the mixture as a cross-linking agent, stirred to form a homogeneous solution, and reacted at 60 °C for 4 h to make it fully cross-linking. The final product was washed with distilled water to remove the unreacted GA, and the composite GL-CS was obtained by freeze-drying for 12 h.

Chitosan-kaolin composite (TGL-CS) by click chemistry method. 59.5 cm^3 of anhydrous C_2H_5OH, 10.5 cm^3 of ultrapure water, 0.600 cm^3 of ammonia and 0.42 g of 3-mercaptopropyltriethoxysilane were added to a 100 cm^3 three-necked flask and heated in a water bath for 3 h. Then it was cooled to room temperature, stirred, 1 g of GL was added, and nitrogen was introduced at one end of the three-necked flask for 6 h. After washing with ethanol and ultrapure water 3 times, the mixture was centrifuged, and finally vacuum freeze-dried at 50 °C for 12 h to obtain thiolated kaolin (TGL). TGL (0.6 g), 2-ethylacrolein (0.3 g) and dimethylolpropionic acid (0.02 g) were dissolved in 20 cm^3 of tetrahydrofuran (THF) and irradiated under UV lamp for 0.5 h. After removing THF, the product AGL was obtained by washing with methanol, then 0.3 g chitosan was added to 20 cm^3 acetic acid solution (2%), and AGL (1.0 g) was added under severe stirring. After stirring at 40 °C for 5 h, TGL-CS was obtained by washing with distilled water and ethanol, vacuum filtration, and freeze-drying for 12 h.

The surface morphology of GL-CS and TGL-CS was analyzed by Gemini300 scanning electron microscope (C. Zeiss, Jena).

Batch adsorption experiments. 0.05 g of adsorbents (GL-CS and TGL-CS) were weighed in a 250 cm^3 conical flask containing 100 cm^3 of lead ion solution. Then, the batch adsorption studies were conducted for various pH (2–6), adsorbent dosage (0.025–0.2 g/dm^3), initial metal ion concentration (10–200 mg/dm^3), contact time (0–1440 min) and temperature (15–55 °C). All batch experiments were conducted in an oscillating incubator (ZQTY-70N) at a constant speed of 120 rpm for about 24 h at 25 °C). Then, the supernatant in conical flasks was filtered through a filter membrane with a pore size of 0.45 μm, and the concentration of Pb^{2+} in the filtrate was determined by flame atomic absorption spectrophotometry (novAA350). Each group of experimental treatment was set up 3 replicates. The adsorption capacity and removal rate of Pb^{2+} were:

- Adsorption capacity

$$q_e = \frac{C_0 - C_e}{M} \times V \tag{1}$$

- Removal rate

$$E = \frac{C_0 - C_e}{C_0} \times 100\% \tag{2}$$

where q_e is the maximum adsorption capacity, mg/g, C_0 is the initial content of Pb^{2+} in aqueous solution, C_e is the content of Pb^{2+} in aqueous solution after adsorption, mg/dm^3, M is the mass of the adsorbent, g, V is the solution volume, dm^3.

3. RESULTS AND DISCUSSION

3.1. SCANNING ELECTRON MICROSCOPY (SEM)

The scanning electron microscope images of GL-CS and TGL-CS at various magnifications are shown in Fig. 1. GL-CS and TGL-CS have different morphologies. The characteristics of GL-CS are blocky, smooth shape, flaky particles adhered to the surface, and no obvious pore structure is visible (Fig. 1a). After magnification (Fig. 1b), it can be seen that the particles are closely distributed, the specific surface area is small, the pores are less and the distribution is uneven. The morphology of TGL-CS is irregular, with more particles attached to the surface, irregular in size, which makes the surface rougher (Fig. 1c). After magnification (Fig. 1d), it can be seen that a large number of pores are formed inside the TGL-CS particles, showing a dense porous three-dimensional structure, increasing the specific surface area, increasing the contact area with Pb^2 (cf. [18]). Comparing the two materials, it can be seen that GL-CS has fewer pores,

TGL-CS has more pores, and a more complex structure. It can be explained that click reactions can efficiently realize the synthesis of polymers [19].

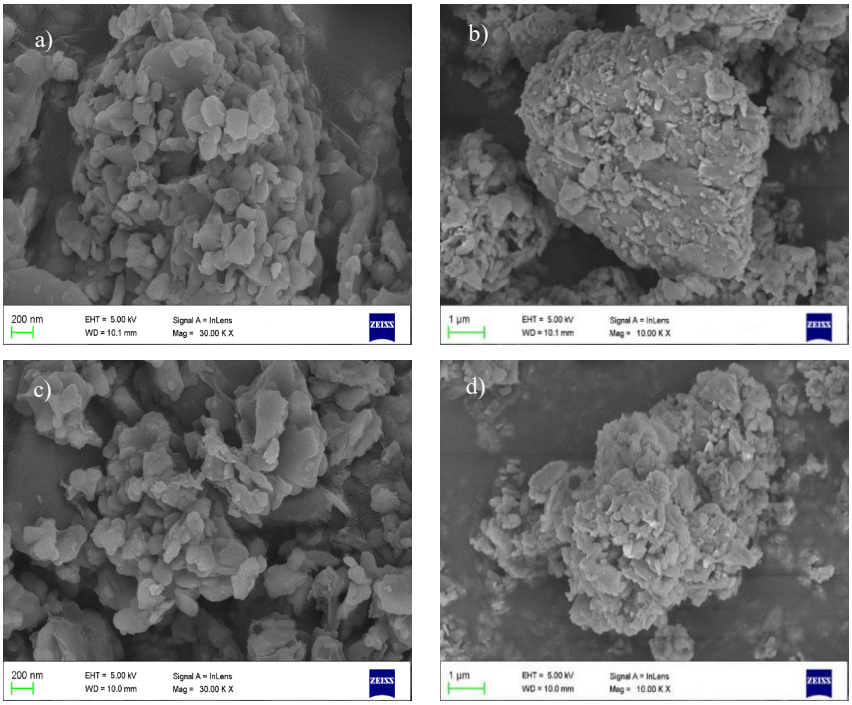

Fig 1. Scanning electron micrographs of GL-CS and TGL-CS:
a) GL-CS (10.00 KX), b) GL-CS (30.00 KX), c) TGL-CS (10.00 KX), d) TGL-CS (30.00 KX)

3.2. EFFECTS OF ADSORPTION TIME, pH, ADSORBENT DOSAGE, Pb^{2+} CONCENTRATION, AND TEMPERATURE

In the first 300 min of the reaction, the adsorbed amount of Pb^{2+} by the two materials increased at a high rate (Fig. 2). As time continued to increase, the adsorption rate of Pb^{2+} remained unchanged [20]. GL-CS reached equilibrium within 6 h, and the equilibrium adsorption capacity was 52.871 mg/g, while TGL-CS reached equilibrium within 4 h, and the equilibrium adsorption capacity was 76.159 mg/dm^3. It shows that the adsorbent TGL-CS prepared by click reaction improved the adsorption rate and significantly reduced the time cost of adsorption compared with GL-CS.

At pH 2–4, the changing trend of the adsorption capacity of GL-CS and TGL-CS is the same, both reaching the highest at pH 4 (Fig. 3). TGL-CS increases the adsorption capacity more at pH 3–4, and the decrease of adsorption capacity of GL-CS was greater at pH 4–5. Therefore, the adsorption capacity of TGL-CS can be significantly improved with the increase of pH, while the adsorption capacity of GL-CS changes

slightly, and the adsorption capacity decreases significantly with the increase of pH. This is because many active functional groups such as amino groups and aldehyde groups are introduced during the preparation of TGL-CS by click reaction, and these functional groups can improve the adsorption capacity of heavy metal ions so that Pb^{2+} can be effectively adsorbed. As the pH continues to increase, the metal ions are easily precipitated, so that the concentration of metal ions is reduced, and the adsorption amount is also reduced. Similar results on various adsorbents were reported by numerous researchers [21, 22].

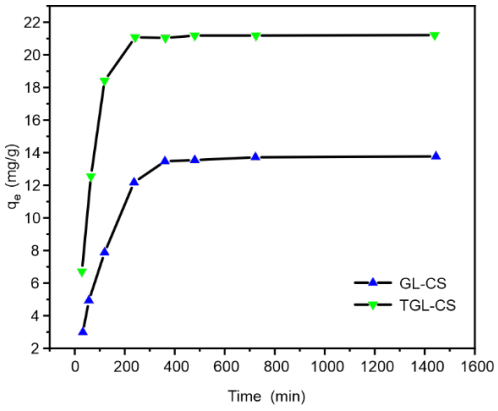

Fig. 2. Effect of time on adsorption of GL-CS and TGL-CS; pH 4, Pb^{2+} concentration 20 mg/dm^3, adsorbent dosage 0.05 g/dm^3, 25 °C

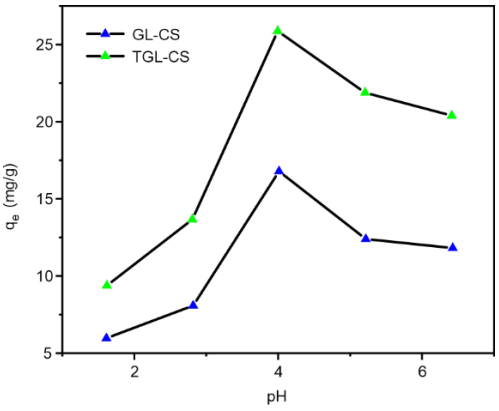

Fig 3. Effect of pH on adsorption of GL-CS and TGL-CS; contact time 24 h, Pb^{2+} concentration 20 mg/dm^3, adsorbent dosage 0.05 g/dm^3, 25 °C

When the amount of adsorbent increased from 0.01 to 0.05 g/dm^3, the adsorption capacity and removal rate of GL-CS and TGL-CS increased and reached the highest value at 0.05 g/dm^3. Then the adsorption capacity of the two adsorbents decreased significantly, while the removal rate remained stable [23, 24]. This is because the adsorption sites are continuously occupied and gradually saturated so that the adsorption rate gradually decreases to a constant value. At 0.01–0.05 g/dm^3, the growth rate of adsorption capacity of TGL-CS was significantly greater than that of GL-CS, and then the downward trend was consistent with the increase of the dosage. The adsorption rate of TGL-CS is faster than that of GL-CS, and rapid adsorption can be achieved in a short time. The click reaction introduces a large number of functional groups, which further improves the adsorption capacity. More adsorption sites can quickly combine with Pb^{2+}. It seems that TGL-CS had better adsorption capacity and percentage removal efficiency as compared with GL-CS. The adsorption capacity of the two materials to lead ions is positively correlated with the initial concentration of lead ions. At a high concentration of Pb^{2+} ions, the adsorption capacity tends to be stable.

The experimental results of Atif et al. [25] also proved this point. GL-CS reached an adsorption saturation state when the concentration of Pb^{2+} was 100 mg/dm^3, and the adsorption capacity was 52.871 mg/g, while TGL-CS reached equilibrium at 150 mg/dm^3, and the adsorption capacity was 76.159 mg/g. The adsorption capacity of TGL-CS is larger and the adsorption performance is better than that of GL-CS as $–NH_2$ and –OH groups in the product of the cross-linking reaction are reduced, and the click reaction can be chemically modified based on the cross-linking productintroduced amino-, aldehyde-, and other groups so that the adsorption performance is significantly improved.

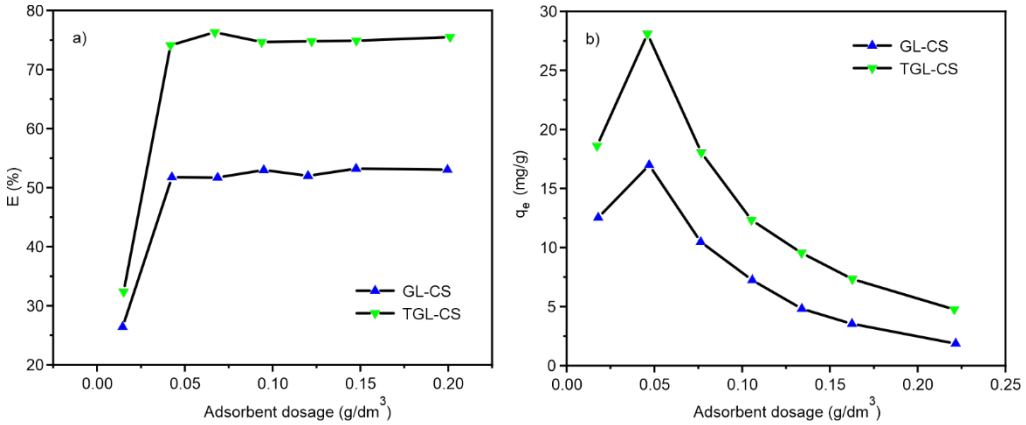

Fig. 4. Effect of adsorbent dosage on adsorption of GL-CS and TGL-CS: a) adsorption capacity trend diagram, b) removal rate trend diagram; contact time 24 h, Pb^{2+} concentration 20 mg/dm^3, pH 4, 25 °C

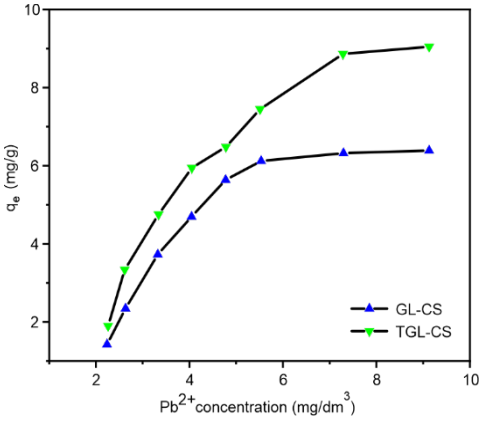

Fig. 5. Effect of initial Pb^{2+} concentration on adsorption of GL-CS and TGL-CS; contact time 24 h, pH 4, adsorbent dosage 0.05 g/dm^3, 25 °C

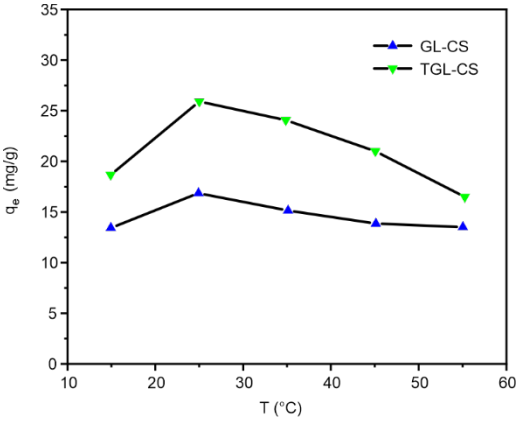

Fig. 6. Effect of temperature on adsorption of GL-CS and TGL-CS; contact time 24 h, pH 4, adsorbent dosage 0.05 g/dm^3, Pb^{2+} concentration 20 mg/dm^3

When the temperature increases from 15 °C to 25 °C, the adsorption capacity of the two materials increases, and when the temperature continues to increase, their adsorption capacity gradually decreases (Fig. 6). The adsorption capacity of TGL-CS strongly depends on temperature, and it is lower than the initial adsorption capacity at 55 °C. The adsorption capacity of GL-CS did not change much and finally maintained the same as the initial adsorption capacity. This proves that TGL-CS is more affected by temperature than GL-CS, and the properties of GL-CS will be relatively stable. The reason may be that the specific surface area of TGL-CS particles is larger, and the reaction process with Pb^{2+} in the solution may be more rapid. When the temperature increases, the structure of the particles is destroyed, and the thermal motion of the molecules will gradually increase, which will damage the existing adsorption equilibrium state. The optimum temperature of the final adsorbent is 25 °C.

3.3. ADSORPTION KINETIC MODEL

The experimental data were calculated and analyzed by PFO (quasi-first order kinetic model), PSO (quasi-second order kinetic model), and intraparticle diffusion model. The kinetic equations of the three models are:

- Quasi-first order kinetic model

$$\ln\left(q_e - q_t\right) = \ln q_e - k_1 t \tag{3}$$

- Pseudo-second order kinetics model

$$\frac{t}{q_t} = \frac{1}{k_2 q_e^2} + \frac{1}{q_e} t \tag{4}$$

- Intraparticle diffusion model

$$q_t = k_p t^{0.5} + C \tag{5}$$

t is adsorption contact time, min, k_1 is PFO parameter, min^{-1}, k_2 is a PSO parameter, g/(mg·min), k_p is the intraparticle diffusion constant, $mg/(g \cdot min)^{-0.5}$, C is a factor dependent on the thickness of the boundary layer. The larger the interface, the greater the boundary layer effect. The fitting results and parameters are shown in Figs. 7–9 and Tables 1 and 2.

By comparing Figs. 7 and 8 and parameters in Table 1, it can be seen that the adsorption process may be better described by pseudo-second order kinetics. The correlation coefficient R^2 of the two adsorbents is greater than 0.99. This means that the adsorption process of Pb^{2+} by TGL-CS and GL-CS meets the requirements of pseudo-second order kinetic equation. It shows that the adsorption process of these two adsorbents is mainly carried out by chemical adsorption.

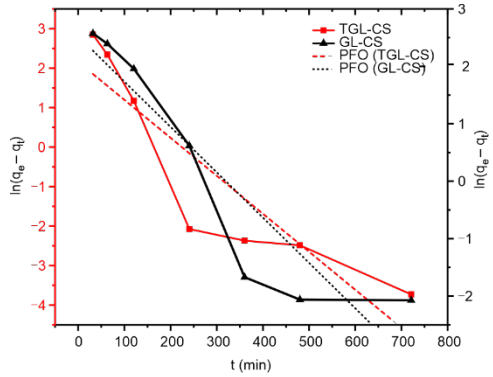

Fig. 7. The pseudo-first order kinetic fitting graph of Pb^{2+}

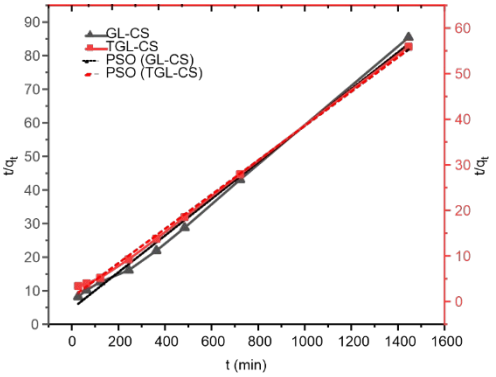

Fig. 8. The pseudo-second order kinetic fitting graph of Pb^{2+}

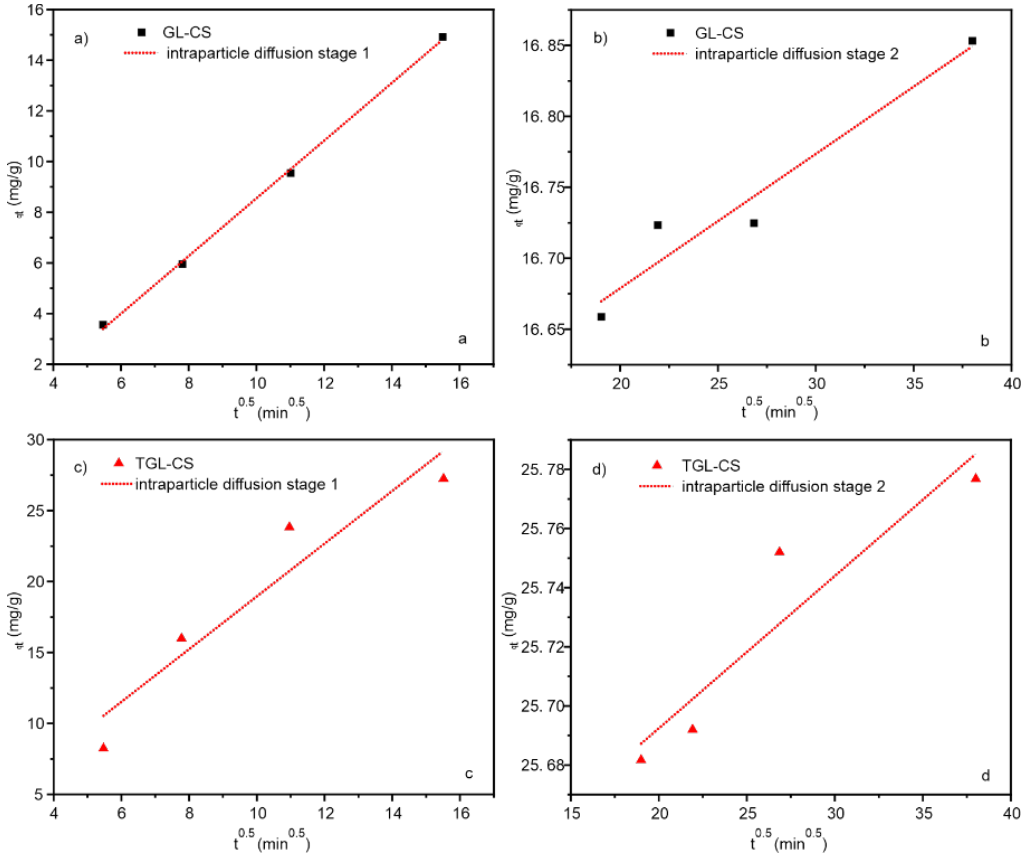

Fig. 9. Fitting diagram of Pb^{2+} intraparticle diffusion models:
GL-CS intraparticle diffusion stages 1 (a), and 2 (b), TGL-CS intraparticle diffusion stages 1 (c) and 2 (d)

Table 1

Pseudo-first order and pseudo-second order adsorption kinetic parameters of the system

Adsorbent	Quasi-first order kinetics			Pseudo-second order kinetics		
	k_1 [min^{-1}]	q_e [mg/g]	R^2	k_2 [g/(mg/min)]	q_e [mg/g]	R^2
GL-CS	0.0079	12.403	0.8561	$6.7*10^{-4}$	18.215	0.9936
TGL-CS	0.0096	8.685	0.8238	0.001	26.596	0.9982

Table 2

Two-stage fitting parameters of intraparticle diffusion kinetics of the system

Adsorbent	Intraparticle diffusion stage 1			Intraparticle diffusion stage 2		
	K_{p1} [$mg/(g\cdot min)^{-0.5}$]	C_1	R^2	K_{p2} [$mg/(g\cdot min)^{-0.5}$]	C_2	R^2
GL-CS	1.1331	–2.6658	0.9992	0.0094	16.491	0.943
TGL-CS	1.7043	1.0063	0.9099	0.0051	25.59	0.8749

The first stage of the intraparticle diffusion model is the adsorption of Pb^{2+} on the surface of GL-CS and TGL-CS adsorbents, and the second stage is the interparticle diffusion of Pb^{2+} on GL-CS and TGL-CS (Fig. 9). From Table 2, the fitting correlation coefficients in stage 1 are all above 0.9, indicating a high degree of fitting.

In stage 2, the R^2 of GL-CS and TGL-CS were 0.943 and 0.8749, respectively, and the fitting degree of GL-CS was better than that of TGL-CS. Comparing the fitting parameters and the thickness of the boundary layer, it was found that the fitting parameters of the two materials increased and the thickness of the boundary layer decreased, indicating that the resistance in the adsorption process gradually increased [26], which may be the reason for affecting the adsorption efficiency.

3.4. ADSORPTION ISOTHERM MODEL

The equations of the three examined isotherms are as follows:

- Langmuir adsorption isotherm

$$\frac{C_e}{q_e} = \frac{1}{k_L q_{e\max}} + \frac{C_e}{q_{e\max}} \tag{6}$$

- Freundlich adsorption isotherm

$$\log q_e = \log K_F + \frac{1}{n}\log C_e \tag{7}$$

- Temkin adsorption isotherm

$$q_e = \frac{R_g T}{b_T} \ln A_T + \frac{RT}{b_T} \ln C_e \tag{8}$$

where C_e is the initial concentration of heavy metal ions, mg/dm^3, q_e is the equilibrium adsorption capacity, mg/g, $q_{e\max}$ is the theoretical maximum adsorption capacity, mg/g, k_L is the Langmuir adsorption equilibrium constant, dm^3/mg, K_F, dm^3/mg, and n are the Freundlich constants, b_T is the Temkin constant related to the adsorption heat, J/mol, A_T is the Temkin isothermal equilibrium binding constant, dm^3/g, R_g is the gas constant, and T is the absolute temperature.

The fitting results of Langmuir, Freundlich, and Temkin isothermal models are shown in Fig. 10, and the calculated parameters are given in Table 3. The R^2 of the Langmuir adsorption model is closer to 1 than the two remaining. Therefore, the adsorption of Pb^{2+} on GL-CS and TGL-CS is mainly single molecule adsorption; the adsorption mechanism is mainly chemical adsorption. It can be seen from the R^2 of the two materials that the adsorption performance of TGL-CS is better than that of GL-CS.

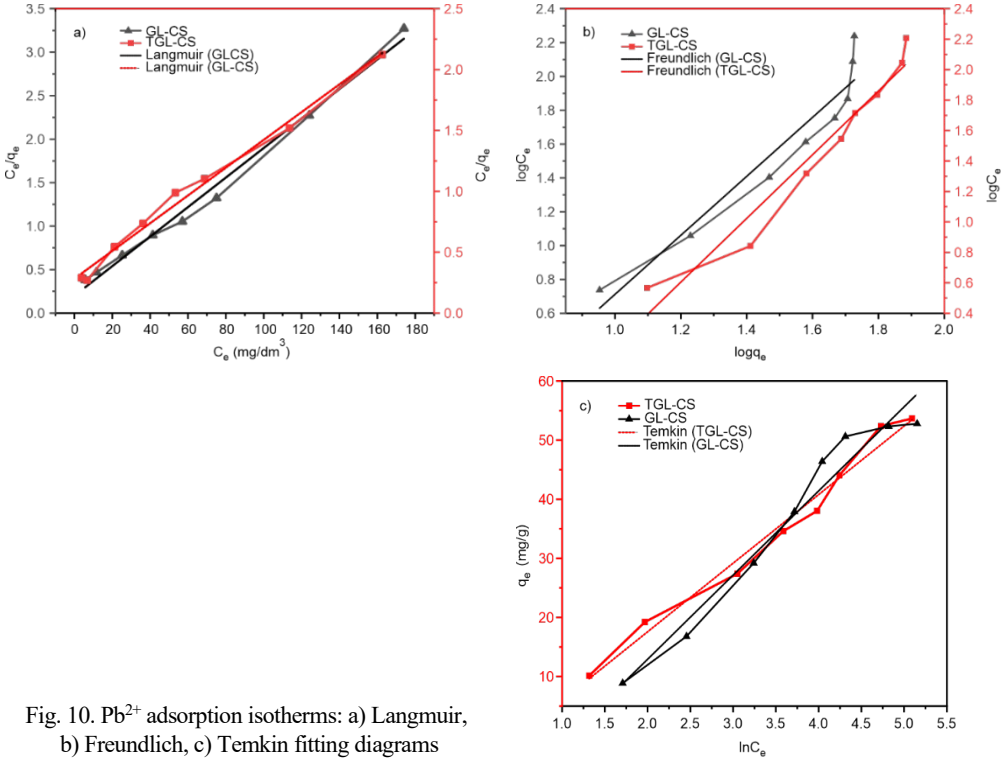

Fig. 10. Pb^{2+} adsorption isotherms: a) Langmuir, b) Freundlich, c) Temkin fitting diagrams

Table 3

Adsorption isotherm parameters of Pb^{2+}

Isotherm type	Parameter	Adsorbent	
		GL-CS	TGL-CS
Langmuir	$q_{e\,max}$, mg/g	63.96	87.72
	K_L, dm^3/mg	0.0356	0.0395
	R^2	0.9906	0.9903
Freundlich	K_F, (mg/g)$(dm^3/mg)^{1/n}$	0.0944	0.0121
	$1/n$	0.5276	0.4519
	R^2	0.9197	0.9512
Temkin	b_T, J/mol	173.34	146.12
	A_T, dm^3/g	0.339	0.542
	R^2	0.9636	0.9838

3.5. ADSORPTION THERMODYNAMIC PARAMETERS

The thermodynamic parameters such as changes of enthalpy (ΔH), entropy (ΔS) and Gibbs free energy (ΔG) may be calculated from the following:

$$K_D = \frac{q_e}{C_e} \tag{9}$$

$$\Delta G = -R_g T \ln K_D \tag{10}$$

$$\ln K_D = \frac{\Delta S}{R_g} - \frac{\Delta H}{R_g T} \tag{11}$$

where K_D is the distribution coefficient, R_g is the gas constant, T is the absolute temperature, K, the values of ΔS and ΔH are determined by the slope and intercept of the diagram $\ln K_D = f(1/T)$.

Table 4

Thermodynamic parameters of Pb^{2+} adsorption

Adsorbent	ΔG [kJ/mol] Temperature [K]					ΔH [kJ/mol]	ΔS [J/(mol·K)]
	288.15	298.15	308.15	318.15	328.15		
GL–CS	–0.048	–0.932	–0.509	–0.137	–0.063	–9.86	–30.2
TGL–CS	–1.349	–3.192	–2.811	–2.055	–0.887	–25.9	–75.686

The adsorption thermodynamic parameters for GL-CS and TGL-CS are given in Table 4. The ΔG values at all temperatures are negative, which proves that the examined

adsorption process is spontaneous; the ΔH values (−9.86 and −25.9 kJ/mol) are also negative, indicating that the adsorption process is exothermic [27, 28]. Similarly, the negative ΔS values (−30.2 and −75.686 J/(mol·K), respectively, indicate that the solute molecules were adsorbed when they were transferred to the solid surface, reducing their degree of freedom, accompanied by a decrease in entropy during the adsorption process [29]. The ΔS value for the TGL-CS–Pb^{2+} system is small, suggesting that its solute molecules are adsorbed in large quantities and less desorbed, which also proves its strong adsorption capacity.

4. CONCLUSIONS

The properties of two kinds of kaolin-chitosan composites (GL-CS and TGL-CS) prepared by cross-linking and click reaction methods were compared. Both have a dense porous three-dimensional structure, but the structural pores of TGL-CS are denser and the distribution of adsorption sites is more uniform, which reflects the advantages of click reaction and can effectively improve the adsorption capacity of the adsorbent. Batch adsorption experiments showed that the adsorption performance of kaolin-chitosan composites prepared by the click reaction method was higher than that of kaolin-chitosan composites prepared by the cross-linking method. With the increase of pH, adsorbent dosage, initial concentration, and time, the adsorption capacity and adsorption rate of TGL-CS were greatly improved compared with GL-CS. With the increase of temperature, the adsorption performance of TGL-CS was unstable, and the adsorption capacity decreased significantly. Although the adsorption capacity of GL-CS is small, it is stable. The adsorption mechanism of GL-CS and TGL-CS is similar, and the adsorption process is mainly based on single-molecule adsorption. The adsorption mechanism is mainly chemical adsorption. The fitting degree of the two materials is high, and the factors affecting the diffusion rate are not unique; the adsorption process is spontaneous and exothermic, and the comparison of ΔS values shows that the adsorption performance of TGL-CS is stronger. The kaolin-chitosan composite prepared by click reaction has a better effect.

ACKNOWLEDGEMENTS

We are sincerely grateful to the reviewers and the editor for their useful comments that helped us to improve the quality of our study. This work was supported by the Science and Technology Research Project of the Education Department of Hubei Province under Grant number B2022013 and Outstanding Young and Middleaged Scientific and Technological Innovation Team Plan in Hubei Province under grant number T2020002.

REFERENCES

[1] BRIFFA J., SINAGRA E., BLUNDELL R., *Heavy metal pollution in the environment and their toxicological effects on humans*, Heliyon, 2020, 6, e04691. DOI: 10.1016/j.heliyon.2020.e04691.

[2] ADNAN M., XIAO B., XIAO P., ZHAO P., LI R., BIBI S., *Research progress on heavy metals pollution in the soil of smelting sites in China*, Toxics, 2022, 10. DOI: 10.3390/toxics10050231.

[3] LU R., FU J., WANG C., QIU C., *Research progress on the characteristics of heavy metal transfer and transformation in municipal sludge treatment*, J. Environ. Eng. Techn., 2023, 13 (01), 318–324. DOI: 10.12153 /j.issn. 1674-991X.20210762.

[4] SHI J.D., ZHAO D., REN F.T., HUANG L., *Spatiotemporal variation of soil heavy metals in China. The pollution status and risk assessment*, Sci. Total Environ., 2023, 871. DOI: 10.1016/j.scitotenv. 2023. 161768.

[5] IFTIKHAR A., UMAIR A., LARAIB M. et al., *Treatment methods for lead removal from* wastewater, [In:] *Lead Toxicity: Challenges and Solution*, N. Kumor, A.H. Jha (Eds.), Springer Nature, Switzerland, 2023, 197–226. DOI: 10.1007/978-3-031-37327-5_10.

[6] SHI R., *Study on adsorption performance ofdiatomite adsorbent for heavy metal ions in water*, 2021. DOI: 10.27671/d.cnki.gcjtc.2021.000583.

[7] NING Z., ALHADI I., YING L., HUIHUI W., HAN G., PENG M., QIANG M., YUBING S., *Recent investigations and progress in environmental remediation by using covalent organic framework-based adsorption method. A review*, J. Clean. Prod., 2020, 277, 123360. DOI: 10.1016/j.jclepro.2020.123360.

[8] KAYALVIZHI K., ALHAJI N.M.I., SARAVANAKKUMAR D., S BEER M., KAVIYARASU K., AYESHAMARIAM A., AMAL M.AL.-M., ABDELGAWWAD M.R., ELSHIH M.S., *Adsorption of copper and nickel by using sawdust chitosan nanocomposite beads. A kinetic and thermodynamic study*, Environ. Res., 2022, 203, 111814. DOI: 10.1016/j.envres.2021.111814.

[9] JI Z., ZHANG Y.S, WANG H.C., LI C., *Research progress in the removal of heavy metals by modified chitosan*, Tens. Surf. Det., 2022, 59 (4), 281–293. DOI: 10.1515/tsd-2021-2414.

[10] ADI L., GUO Z., HU Y., *Research progress on modification technology of chitosan and its application in water treatment*, Cont. Chem. Ind., 2022, 51 (11), 2732–2735, 2758. DOI: 10.13840/j.cnki.cn21 -1457/tq.2022.11.005.

[11] FENG S., ZU Y., ZHAO C., GONG M., XIN Y., JIANG W., WANG D., *Research progress on adsorption of heavy metal ions in water by modified chitosan adsorbent*, Pol. Mate. Sci. Eng., 2022, 38 (8), 185–190. DOI: 10.16865/j.cnki.1000-7555.2022.0184.

[12] ZHANG S., LU F., JIANG L., *Electrochemical properties of kaolin interface and its adsorption of heavy metals*, J. Shandong Agricultural University (Natural Science Edition), 2014, 45 (5), 675–679, 685. DOI: 10.13840/j.cnki.cn21-1457/tq.2019.08.007.

[13] CHAI J., AU P., MUBARAK N., KHALID M., NG W., JAGADISH P., WALVEKAR R., ABDULLAH E., Adsorption *of heavy metal from industrial wastewater onto low-cost malaysian kaolin clay-based adsorbent*, Environ. Sci. Poll. Res., 2020, 27, 13949–13962. DOI: 10.1007/s11356-020-07755-y.

[14] HE G., WANG C., CAO J., FAN L., ZHAO S., CHAI Y., *Carboxymethyl chitosan-kaolinite composite hydrogel for efficient copper ions trapping*, J. Environ. Chem. Eng., 2019, 7, 102953. DOI: 10.1016 /j.jece.2019.102953.

[15] VEDULA S.S., YADAV G.D., *Superior efficacy of biocomposite membranes of chitosan with montmorillonite and kaolin vs pure chitosan for removal of Cu(II) from wastewater*, J. Chem. Sci., 2022, 134 (2), 1–12.

[16] LIU D.-M., DONG C., XU B., *Preparation of magnetic kaolin embedded chitosan beads for efficient removal of hexavalent chromium from aqueous solution*, J. Environ. Chem. Eng., 2021, 9 (4), 105438. DOI: 10.1016/j.jece.2021.105438.

[17] ZHOU Y., LIU Q., SUN J., HUANG T., *Study on adsorption of phosphorus from wastewater by chitosan/kaolin composite*, China Biogas, 2022, 40 (6). DOI: 10.1016/j.cnki.1000-1166.2022060043.

[18] YANG W., XIE H., *Adsorption of heavy metal ions in electroplating wastewater by chitosan intercalated kaolin*, Mater. Prot., 2016, 49 (11), 75–78. DOI: 10.16577/j.cnki.42-1215/tb.2016.11.021.

[19] YAP P.L., AUYOONG Y.L., HASSAN K., FARIVAR F., TRAN D.N.H., MA J., LOSIC D., *Multithiol functionalized graphene bio-sponge via photoinitiated thiol-ene click chemistry for efficient heavy metal ions adsorption*, Chem. Eng. J., 2020, 395, 124965. DOI: 10.1016/j.cej.2020.124965.

[20] CHEN L., *Preparation of chitosan modified material and its adsorption capacity for heavy metal ions in wastewater*, 2023, 2, 95. DOI: 10.27859/d.cnki.gxhsf.2022.000239.

[21] ELANCHEZHIYAN S.S., KARTHIKEYAN P., RATHINAM K., HASMATH FARZANA M., PARK C.M., *Magnetic kaolinite immobilized chitosan beads for the removal of Pb(II)*, Carb. Polym., 2021, 261, 117892. DOI: 10.1016/j.carbpol.2021.117892.

[22] ANITHA T., SENTHIL KUMAR P., SATHISH KUMAR K., RAMKUMAR B., RAMALINGAM S., *Adsorptive removal of Pb(II) ions from polluted water by newly synthesized chitosan-polyacrylonitrile blend. Equilibrium, kinetic, mechanism and thermodynamic approach*, Proc. Saf. Environ. Prot., 2015, 98, 187–197. DOI: 10.1016/j.psep.2015.07.012.

[23] TANG C., LI S., SHANG K., HUANG L., YANG F., LIU Y., *Study on the performance of kaolin loaded modified chitosan heavy metal adsorbent*, Cont. Chem. Ind., 2019, 48 (8), 1664–1667. DOI: 10.13840/j.cnki.cn21-1457/tq. 2019.08.007.

[24] SUN Y., SHAH K.J., SUN W., ZHENG H., *Performance evaluation of chitosan-based flocculants with good pH*, Sep. Purif. Techn., 2019, 215, 208–216. DOI: 10.1016/j.seppur.2019.01.017.

[25] ATIF S., WANG J.H., SUN T.T., TONGTONG S., FAISAL S., MUHAMMAD H., SILI L., *Enhanced and selective adsorption of copper ions from acidic conditions by diethylenetriaminepentaacetic acid-chitosan sewage sludge composite*, J. Environ. Chem. Eng., 2020, 8, 104430. DOI: 10.1016/j.jece.2020.104430.

[26] YANG K., JIANG Y., YANG J., LIN D., *Correlations and adsorption mechanisms of aromatic compounds on biochars produced from various biomass at 700 °C*, Environ. Poll., 2018, 233, 64–70. DOI: 10.1016/j.envpol.2017.10.035.

[27] ZHANG D., XIE Y., SHI H., ZHUO X., LI X., *Kinetics and thermodynamics studies on Ni^{2+} adsorption by modified chitosan*, J. Shaoyang University (Natural Science Edition), 2019, 16 (03), 68–75. DOI: 1672-7010(2019)03-0068-08.

[28] YANG J.B., HUANG B., LIN M.Z., *Adsorption of hexavalent chromium from aqueous solution by a chitosan/bentonite composite: isotherm, kinetics, and thermodynamics studies*, J. Chem. Eng. Data, 2020, 65, 2751–2763. DOI: 10.1021/acs.jced.0c00085.

[29] HUANG Z., NING Z., XIAO T., ZHAO Y., LIU Y., WU S., LAN X., *Comparative study on the removal of Sb(V) from water by different adsorbents*, Earth and Environ., 2017, 45 (5), 523–530. DOI: 10.14050/j.cnki.1672-9250.2017.05.005.